

## Editor Comments:

The Title is a bit awkward. I think it should read “Estimates of late middle Eocene pCO<sub>2</sub> based on stomatal density of modern and fossil *Nageia* leaves”. This better incorporates the contents of the manuscript with correct grammar. Also, I think ~40 Ma is better described as late middle Eocene, and I do not think Gaertner needs inclusion as the genus, while not well known, is well established.

The title has been changed as suggested.

Lines 44-47: This is over-referenced and arguably incorrect. I would just put “In particular, there are few reconstructions for the late middle Eocene.” (And then cite those papers that show this aspect).

Changed as suggested.

Line 128: I think this should be “... into two “sections”, ...” (I assuming here that sections is a biological classification term).

Changed as suggested.

Line 134: Needs space.

Changed as suggested.

Lines 161-162: I think this should be “... surfaces of leaves might be used ...”

Changed as suggested.

Lines 173-174: This should be “... hours, the reaction was stopped when specimen fragments ... and transparent. The ...” (There should be no semicolons in this case).

Changed as suggested.

Line 175: Should be “After, the ...”

Changed as suggested.

Line 178: Needs period as already has an “and” (i.e., “... 30 min). The ...”)

Changed as suggested.

**\*\*A\*\*** Lines 192-197: This needs rewriting as important information is missing. It

should be something like “Further information on the sections is provided by Lie et al. (2015). Importantly, the formations span a depositional age of approximately XX to YY Ma, or late middle Eocene (REF). This has been determined HOW? (1-2 sentences). Now start new paragraph “Macrofossil ...” (Are other approaches the same as for modern leaves? This is not crystal clear right now).

Lines 192-194 are changed as suggested. The approaches for fossil are different from modern ones, so we add “directly” in front of “treated” to make the sentence clearer.

Line 216: Remove space.

Changed as suggested.

Line 229: Spell-out “Figure”

Changed as suggested.

Line 245: Indent paragraph.

Changed as suggested.

Line 293: Should be “For modern Nageia, we find that ... increase, but that ...”

Changed as suggested.

Lines 295-296: Should be “... case has been observed for some flora.”

Changed as suggested.

Line 300: Can remove “herein ...”. Just end the sentence after “cells.”

Changed as suggested.

Line 301: Start new paragraph and indent.

Changed as suggested.

Lines 312-313: Tense. Should be “... was young or mature, or grew in a sunny or shady environment”.

Changed as suggested.

Lines 321-322: Should be “..., which is fairly close to GEOCARB III predictions ...”

Changed as suggested.

Lines 326-327: Should be "... were generally lower than during much of the Cretaceous, but probably also decreased significantly from the early to late Eocene (REF). Here, I would fix the references. For example, two sets of references not needed, and Zachos et al. 2001 does not really discuss pCO<sub>2</sub>.

Changed as suggested.

Lines 330-334: I would change to "However, there is a wide range of estimates for the Eocene (REF)." (Then remove the rest, as it is not really pertinent).

Changed as suggested.

**\*\*B\*\*** Lines 336-380: This needs to be condensed and rewritten. All that should be here are past estimates for the middle to late Eocene, and how the Nageia estimates compare. However, there is a critical piece of information that needs to be tied in with the comment above. The world was dynamic in the Paleogene, including in the late middle Eocene, when the MECO occurred. Thus, the exact age matters, and it is possible that a values may differ because of slight offsets in time.

Changed as suggested.

In addition, we made a few changes as follows:

Line 237-238, add two spaces after "=".

Line 349, we use "to" substitute for "and".

1     ~~The Estimates of late middle Eocene~~ **pCO<sub>2</sub> estimates of the late-**  
2     ~~Eocene in South China~~ **based on stomatal density of modern and**  
3                     **fossil *Nageia Gaertner* leaves**

4  
5                     XIAO-YAN LIU, QI GAO, MENG HAN and JIAN-HUA JIN\*

6  
7     State Key Laboratory of Biocontrol and Guangdong Provincial Key Laboratory of Plant Resources,  
8     School of Life Sciences, Sun Yat-sen University, Guangzhou 510275, China

9  
10    **Abstract:**

11    Atmospheric pCO<sub>2</sub> concentrations have been estimated for intervals of the Eocene  
12    using various models and proxy information. Here we reconstruct late middle Eocene  
13    (~~42.0-38.5~~ 40.3 Ma) pCO<sub>2</sub> based on the fossil leaves of *Nageia maomingensis* Jin et  
14    Liu collected from the Maoming Basin, Guangdong Province, China. We first  
15    determine relationships between atmospheric pCO<sub>2</sub> concentrations, stomatal density  
16    (SD) and stomatal index (SI) using “modern” leaves of *N. motleyi* (Parl.) De Laub, the  
17    nearest living species to the Eocene fossils. This work indicates that the SD inversely  
18    responds to pCO<sub>2</sub>, while SI has almost no relationship with pCO<sub>2</sub>. Eocene pCO<sub>2</sub>  
19    concentrations can be reconstructed based on a regression approach and the stomatal  
20    ratio method by using the SD. The first approach gives a pCO<sub>2</sub> of 351.9 ± 6.6 ppmv,  
21    whereas the one based on stomatal ratio gives a pCO<sub>2</sub> of 537.5 ± 56.5 ppmv. Here, we

\_\_\_\_\_

\*

Correspondence: Jianhua Jin, tel. +86 20 84113348, fax +86 20 84110436, e-mail: lssjhh@mail.sysu.edu.cn

22 explored the potential of *N. maomingensis* in pCO<sub>2</sub> reconstruction and obtained  
23 different results according to different methods, providing a new insight for the  
24 reconstruction of paleoclimate and paleoenvironment in conifers.

25

26 | **Keywords:** pCO<sub>2</sub>, late [middle](#) Eocene, *Nageia*, Maoming Basin, South China.

27

## 28 | **1 Introduction**

29

30 The Eocene (55.8-33.9 Ma) generally was much warmer than present-day, although  
31 temperatures varied significantly across this time interval (Zachos et al., 2008).

32 Climate of the early Eocene was extremely warm, particularly during the early  
33 Eocene Climatic Optimum (EECO; 51 to 53 Ma), and the Paleocene-Eocene Thermal  
34 Maximum (PETM; ~55.9 Ma). However, global climatic conditions cooled  
35 | significantly by the [middle to](#) late Eocene (40 to 36 Ma). Indeed, small, ephemeral  
36 ice-sheets and Arctic sea ice likely existed during the latest Eocene (Moran et al.,  
37 2006; Zachos et al., 2008).

38 Many authors have suggested that changes in temperature during the Phanerozoic  
39 were linked to atmospheric pCO<sub>2</sub> (Petit et al., 1999; Retallack, 2001; Royer, 2006).  
40 Central to these discussions are records across the Eocene, as this epoch spans the last  
41 major change from a “greenhouse” world to an “icehouse” world. The Eocene pCO<sub>2</sub>  
42 record remains incomplete and debated (Kürschner et al., 2001; Royer et al., 2001;  
43 Beerling et al., 2002; Greenwood et al., 2003; Royer, 2003). Most pCO<sub>2</sub>

44 reconstructions have focused on the Cretaceous-Tertiary and Paleocene-Eocene  
45 boundaries (65 to 50 Ma; ~~Koch et al., 1992; Stott, 1992; Sinha and Stott, 1994; Royer~~  
46 ~~et al., 2001; Beerling and Royer, 2002; Nordt et al., 2002; Royer, 2003; Fletcher et al.,~~  
47 ~~2008; Roth Nebelsick et al., 2012; 2014; Grein et al., 2013; Huang et al., 2013;~~  
48 ~~Maxbauer et al., 2014)~~ and the middle Eocene. ~~(Maxbauer et al., 2014), while few~~  
49 ~~reconstructions were conducted at the late Eocene~~ In particular, there are few  
50 reconstructions for the late middle Eocene (Pagani et al., 2005; Maxbauer et al., 2014).

51 In addition, the pCO<sub>2</sub> reconstruction results have varied based on different proxies.  
52 Various methods having been used in pCO<sub>2</sub> reconstruction mainly include the  
53 computer modeling methods: GEOCARB-I, GEOCARB-II, GEOCARB-III,  
54 GEOCARB-SULF and the proxies: ice cores, paleosol carbonate, phytoplankton,  
55 nahcolite, Boron, and stomata parameters.

56 The abundance of stomatal cells can be measured on modern leaves and  
57 well-preserved fossil leaves. Various plants show a negative correlation between  
58 atmospheric CO<sub>2</sub> concentration and stomatal density (SD), stomatal index (SI), or  
59 both. As such, these parameters have been determined in fossil leaves to reconstruct  
60 past pCO<sub>2</sub>; examples include *Ginkgo* (Retallack, 2001, 2009a; Beerling et al., 2002;  
61 Royer, 2003; Kürschner et al., 2008; Smith et al., 2010), *Metasequoia* (Royer, 2003;  
62 Doria et al., 2011), *Taxodium* (Stults et al., 2011), *Betula* (Kürschner et al., 2001; Sun  
63 et al., 2012), *Neolitsea* (Greenwood et al., 2003), and *Quercus* (Kürschner et al., 1996,  
64 2001), *Laurus* and *Ocotea* (Kürschner et al., 2008). Recently, positive correlations  
65 between stomatal index or stomatal frequency and pCO<sub>2</sub> have been reported based on

66 fossil *Typha* and *Quercus* (Bai et al., 2015; Hu et al., 2015). However, the tropical and  
67 subtropical moist broadleaf forest conifer tree *Nageia* has not been used previously in  
68 paleobotanical estimates of pCO<sub>2</sub> concentration.

69 Herein, we firstly document correlations between stomatal properties and  
70 atmospheric CO<sub>2</sub> concentrations using leaves of the extant species *Nageia motleyi*  
71 (Parl.) De Laub. that were collected over the last two centuries. This provides a  
72 training dataset for application to fossil representatives of *Nageia*. We secondly  
73 measure stomatal parameters on fossil *Nageia* leaves from ~~the~~ late middle Eocene of  
74 South China to estimate past CO<sub>2</sub> levels. The work provides further insights for  
75 discussing Eocene climate change.

76

## 77 **2 Background**

78

### 79 **2.1 Stomatal proxy in pCO<sub>2</sub> research**

80

81 Stomatal information gathered from careful examination of leaves has been widely  
82 used for reconstructions of past pCO<sub>2</sub> concentrations (Beerling and Kelly, 1997; Doria  
83 et al., 2011). The three main parameters are stomatal density (SD), which is expressed  
84 as the total number of stomata divided by area, epidermal density (ED), which is  
85 expressed as the total number of epidermal cells per area, and the stomatal index (SI),  
86 which is defined as the percentage of stomata among the total number of cells within  
87 an area [ $SI = SD \times 100 / (SD + ED)$ ]. Woodward (1987) considered that both SD and SI

88 had inverse relationships with atmospheric CO<sub>2</sub> during the development of the leaves.  
89 Subsequently, McElwain (1998) created the stomatal ratio (SR) method to reconstruct  
90 pCO<sub>2</sub>. SR is a ratio of the stomatal density or index of a fossil [*SD<sub>(f)</sub>* or *SI<sub>(f)</sub>*] to that of  
91 corresponding nearest living equivalent [*SD<sub>(e)</sub>* or *SI<sub>(e)</sub>*], expressed as follows:

$$92 \quad SR = SI_{(e)} / SI_{(f)} \quad (1)$$

93 The stomatal ratio method is a semi-quantitative method of reconstructing pCO<sub>2</sub>  
94 concentrations under certain standardizations. An example is the “Carboniferous  
95 standardization” (Chaloner and McElwain, 1997), where one stomatal ratio unit  
96 equals two RCO<sub>2</sub> units:

$$97 \quad SR = 2 \text{ RCO}_2 \quad (2)$$

98 and the value of RCO<sub>2</sub> is the pCO<sub>2</sub> level divided by the pre-industrial atmospheric  
99 level (PIL) of 300 ppm (McElwain, 1998) or that of the year when the nearest living  
100 equivalent (NLE) was collected (Berner, 1994; McElwain, 1998):

$$101 \quad \text{RCO}_2 = C_{(f)} / 300 \text{ or } \text{RCO}_2 = C_{(f)} / C_{(e)} \quad (3)$$

102 The estimated pCO<sub>2</sub> level can then be expressed as follows:

$$103 \quad C_{(f)} = 0.5 \times C_{(e)} \times SD_{(e)} / SD_{(f)} \text{ or } C_{(f)} = 0.5 \times C_{(e)} \times SI_{(e)} / SI_{(f)} \quad (4)$$

104 where *C<sub>(f)</sub>* is the pCO<sub>2</sub> represented by the fossil leaf, and *C<sub>(e)</sub>* is the atmospheric CO<sub>2</sub>  
105 of the year when the leaf of the NLE species was collected (McElwain and Chaloner,  
106 1995, 1996; McElwain 1998). The equation adapts to the pCO<sub>2</sub> concentration prior to  
107 Cenozoic.

108 Another standardization, the “Recent standardization” (McElwain, 1998), is  
109 expressed as one stomatal ratio unit being equal to one RCO<sub>2</sub> unit:



110  $SR = 1 RCO_2$  (5)

111 According to the equations stated above, the  $pCO_2$  concentration can be expressed  
112 as:

113  $C_{(f)} = C_e \times SD_{(e)} / SD_{(f)}$  or  $C_{(f)} = C_e \times SI_{(e)} / SI_{(f)}$  (6)

114 This standardization is usually used for reconstruction based on Cenozoic fossils  
115 (Chaloner and McElwain, 1997; McElwain, 1998; Beerling and Royer, 2002).

116 Kouwenberg et al. (2003) proposed some special stomatal quantification methods  
117 for conifer leaves with stomata arranged in rows. The stomatal number per Length  
118 (SNL) is expressed as the number of abaxial stomata plus the number of adaxial  
119 stomata divided by leaf length in millimeters. Stomatal rows (SRO) is expressed as  
120 the number of stomatal rows in both stomatal bands. Stomatal density per length  
121 (SDL) is expressed as the equation  $SDL = SD \times SRO$ . True stomatal density per  
122 length (TSDL) is expressed as the equation  $TSDL = SD \times \text{band width (in millimeters)}$ .  
123 The band width on *Nageia motleyi* leaves was measured as leaf blade width.

124

## 125 **2.2 Review of extant and fossil *Nageia***

126

127 The genus *Nageia*, including seven living species, is a special group of  
128 Podocarpaceae, a large family of conifers mainly distributed in the southern  
129 hemisphere. *Nageia* has broadly ovate-elliptic to oblong-lanceolate, multiveined  
130 (without a midvein), spirally arranged or in decussate, and opposite or subopposite  
131 leaves (Cheng et al., 1978; Fu et al., 1999). Generally, *Nageia* is divided into two

132 | sections. *Nageia* Sect. *Nageia* and *Nageia* Sect. *Dammaroideae* (Mill 1999, 2001).  
133 Both sections are mainly distributed in southeast Asia and Australasia from north  
134 latitude 30 ° to nearly the equator (Fu, 1992; Fig. 1). Four species of the *N.* section  
135 *Nageia* -- *Nageia nagi* (Thunberg) O. Kuntze, *N. fleuryi* (Hickel) De Laub., *N.*  
136 *formosensis* (Dummer) C. N. Page, and *N. nankoensis* (Hayata) R. R. Mill -- have  
137 | hypostomatic leaves where stomata only occur on the abaxial side. One species of this  
138 section -- *N. maxima* (De Laub.) De Laub. -- is characterized by amphistomatic leaves,  
139 but where only a few stomata are found on the adaxial side (Hill and Pole, 1992; Sun,  
140 2008). Both *N. wallichiana* (Presl) O. Kuntze and *N. motleyi* of the *N.* section  
141 *Dammaroideae* are amphistomatic with abundant stomata distributed on both sides of  
142 the leaf. This is especially true for *N. motleyi*, which has approximately equal stomata  
143 numbers on both surfaces (Hill and Pole, 1992; Sun, 2008).  
144 The fossil record of *Nageia* can be traced back to the Cretaceous. Krassilov (1965)  
145 described *Podocarpus (Nageia) sujfunensis* Krassilov from the Lower Cretaceous of  
146 Far East Russia. Kimura et al. (1988) reported *Podocarpus (Nageia) ryosekiensis*  
147 Kimura, Ohanaet Mimoto, an ultimate leafy branch bearing a seed, from the Early  
148 Barremian in southwestern Japan. In China, a Cretaceous petrified wood, *Podocarpus*  
149 (*Nageia*) *nagi* Pilger, was discovered from the Dabie Mountains in central Henan,  
150 China (Yang et al., 1990). Jin et al. (2010) reported a upper Eocene *Nageia* leaf  
151 named *N. hainanensis* Jin, Qiu, Zhu et Kodrul from the Changchang Basin of Hainan  
152 Island, South China. Recently, Liu et al. (2015) found another leaf species *N.*  
153 | *maomingensis* Jin et Liu from upper middle Eocene of Maoming Basin, South China.

154 Although some of the *Nageia* fossil materials described in the above studies  
155 (Krassilov, 1965; Jin et al., 2010; Liu et al., 2015) have well-preserved cuticles, these  
156 studies are mainly concentrated on morphology, systematics and phytogeography.

157 Here we try to reconstruct the pCO<sub>2</sub> concentration based on stomatal data of  
158 *Nageia maomingensis* Jin et Liu. Among the modern *Nageia* species mentioned above,  
159 *N. motleyi* was considered as the NLE species of *N. maomingensis* (Liu et al., 2015).  
160 However, because of the species-specific inverse relationship between atmospheric  
161 CO<sub>2</sub> partial pressure and SD (Woodward and Bazzaz, 1988), it is necessary to explore  
162 whether the SD and SI of *N. motleyi* show negative correlations with the CO<sub>2</sub>  
163 concentration before applying the stomatal method. Both *N. maomingensis* and *N.*  
164 *motleyi* are amphistomatic, suggesting that both upper and lower surfaces of ~~the leaf~~  
165 are needed leaves might be used to estimate the pCO<sub>2</sub> concentrations.

166

### 167 **3 Material and methods**

168

#### 169 **3.1 Extant leaf preparation**

170

171 We examined 12 specimens of extant *Nageia motleyi* from different herbaria (Table  
172 1). We removed one or two leaves from each specimen, and took three fragments  
173 (0.25 mm<sup>2</sup>) from every leaf (Fig. 2a) and numbered them for analysis.

174 The numbered fragments were boiled for 5-10 min in water. Subsequently, after  
175 being macerated in a mixed solution of 10% acetic acid and 10% H<sub>2</sub>O<sub>2</sub> (1:1) and

176 heated in the thermostatic water bath at 85 C for 8.5 hours; the reaction was stopped  
177 when the specimens fragments turned white and semitransparent. The cuticles were  
178 then rinsed with distilled water until the pH of the water became neutral. After, ~~that~~  
179 the cuticles were treated in Schulze's solution (one part of potassium chlorate  
180 saturated solution and three part of concentrated nitric acid) for 30 min, rinsed in  
181 water, and then treated with 8% KOH (up to 30 min). ~~and the~~ The abaxial and adaxial  
182 cuticles were separated with a hair mounted on needle. Finally, the cuticles were  
183 stained with 1% Safranin T alcoholic solution for 5 min, sealed with Neutral Balsam  
184 and observed under LM.

185

### 186 3.2 Fossil leaf preparation

187

188 Maoming Basin (21 °42'33.2"N, 110 °53'19.4"E) is located in southwestern  
189 Guangdong, South China including Cretaceous and Tertiary strata. Tertiary strata are  
190 fluvial and lacustrine sedimentary units, divided into the Gaopengling, Laohuling,  
191 Shangcun, Huangniuling and Youganwo formations in descending order, aged from  
192 late Eocene to early Oligocene (Wang et al., 1994).

193 Four fossil leaves of *Nageia maomingensis* were recovered from the Youganwo  
194 (MMJ1-001) and Huangniuling (MMJ2-003, MMJ2-004 and MMJ3-003) formations  
195 of Maoming Basin, South China (~~Fig. 1B, 1C in Liu et al., 2015~~). Further information  
196 on the sections is provided by Liu et al. (2015). Importantly, the formations span a  
197 depositional age of approximately 42.0 to 38.5 Ma which was considered as late

198 ~~Eocene by Wang et al. (1994), but it can be recognized as late middle Eocene~~  
199 ~~according to Walker and Geissman (2009). The age from Youganwo to Huangniuling~~  
200 ~~formations is late Eocene (~40.3 Ma). Precise information regarding locations is~~  
201 ~~provided by Liu et al., (2015).~~

202 Macrofossil cuticular fragments were taken from the middle part of each fossil leaf  
203 (Fig. 2c) and directly treated with Schulze's solution for approximately 1 h and 5–10%  
204 KOH for 30 min (Ye, 1981). The cuticles were observed and photographed under a  
205 Carl Zeiss Axio Scope A1 light microscope (LM). All fossil specimens and cuticle  
206 slides are housed in the Museum of Biology of Sun Yat-sen University, Guangzhou,  
207 China.

### 209 3.3 Stomatal counting strategy and calculation methods

211 The basic stomatal parameters, SD, ED and SI, were counted based on analyzing  
212 pictures taken with a light microscope (LM). A total of 2816 pictures (200×  
213 magnification of Zeiss LM) of cuticles from 21 leaves of *N. motleyi* were counted.  
214 Each counting field was 0.366 mm<sup>2</sup>. We used a standard sampling protocol (Poole and  
215 Kürschner, 1999), counting all full stomata in the image plus stomata straddling the  
216 left and top margins, as presented in Figure 2(b), and (d).

217 The SNL, SRO, SDL, and TSDL were also determined based on LM images. A  
218 total of 2293 pictures (200× magnification of Zeiss LM) of the cuticles from 21 leaves  
219 of *N. motleyi* were counted. Each counting field was 0.366 mm<sup>2</sup>. None of the

220 |    aforementioned counting areas overlapped and they were larger than the minimum  
221 |    area (0.03 mm<sup>2</sup>) for statistics (Poole and Kürschner, 1999). In this study, the stomatal  
222 |    data of both surfaces are applied in pCO<sub>2</sub> reconstruction because both the fossil and  
223 |    NLE species are amphistomatic.

224 |

225 |

## 226 | **4 Results**

227 |

### 228 | **4.1 Correlations between the CO<sub>2</sub> concentrations and stomatal parameters of**

#### 229 | *Nageia motleyi*

230 |

231 |    The SD and SI data of the adaxial sides of *N. motleyi* leaves are presented in Table  
232 |    2. The SDs and SIs average 62.28 mm<sup>-2</sup> and 3.30 %, respectively. However, the SDs  
233 |    and SIs data of the abaxial sides, summarized in Table 3, give higher average values  
234 |    (70.03 mm<sup>-2</sup> in SDs and 3.90 % in SIs) than those from the adaxial sides. The  
235 |    combined SD and SI of the adaxial and abaxial surfaces average 66.14 mm<sup>-2</sup> and  
236 |    3.60 %, respectively (table 4).

237 |    Fig-[ure 3](#) shows the relationships between the stomatal parameters (SD and SI) of  
238 |    modern *N. motleyi* and the atmospheric CO<sub>2</sub> concentration (SD-CO<sub>2</sub> relationship and  
239 |    SI-CO<sub>2</sub> relationship). R<sup>2</sup> values in the SD-CO<sub>2</sub> relationship from the adaxial and  
240 |    abaxial surfaces of *N. motleyi* are up to 0.4667 and 0.3824 (Fig. 3a, b), suggesting that  
241 |    the stomatal densities of *N. motleyi* are inverse to the CO<sub>2</sub> concentrations. However,

242 Fig. 3c and d indicate no relationship between the SIs and CO<sub>2</sub> concentrations for the  
243 extremely low level of the R<sup>2</sup> values (0.2558 and 0.0248). Figs. 3e and 3f based on the  
244 combined data also show that SD inversely responds to the atmospheric CO<sub>2</sub>  
245 concentration (R<sup>2</sup> = 0.4421), while SI has almost no relationship with the atmospheric  
246 CO<sub>2</sub> concentration (R<sup>2</sup> = 0.1177).

247 The mean values of SNL, SDL and TSDL are 9.81, 326.39 and 1226.93 no.·mm<sup>-1</sup>,  
248 respectively (Table 5). Fig. 4 shows the relationships between SNL (SDL, TSDL) and  
249 CO<sub>2</sub> concentrations. The low R<sup>2</sup> values in the Fig. 4a and 4c indicate that SNL (R<sup>2</sup> =  
250 0.0643) and TSDL (R<sup>2</sup> = 0.0788) have no relationship with the CO<sub>2</sub> concentration in  
251 this study. Fig. 4b shows that there is a weak reverse relevance between SDL and the  
252 CO<sub>2</sub> concentration (R<sup>2</sup> = 0.3154).

253 Compared with the SDL method, the SD-based method shows a larger R<sup>2</sup> value,  
254 indicating a stronger relevance between the SD and CO<sub>2</sub> concentrations. In this study,  
255 the pCO<sub>2</sub> is reconstructed based on the regression equations of SD-CO<sub>2</sub> relationship.  
256 Additionally, the stomatal ratio method can be also used in estimating pCO<sub>2</sub>  
257 concentration of ~~the~~ late middle Eocene based on stomatal densities (SDs) of the  
258 fossil species *N. maomingensis* and extant species *N. motleyi*. The SD results of  
259 specimen No. 18328 are selected to reconstruct the pCO<sub>2</sub> concentration, because they  
260 are closest to the fitted equations in Fig. 3. This specimen was collected by Neth. Ind.  
261 For. Service from Riau on Ond. Karimon, Archipel. Ind., Malaysia, in 1934 at an  
262 altitude of 5 m and CO<sub>2</sub> concentration of 306.46 ppmv (Brown, 2010).

263

带格式的：缩进：首行缩进：1 字符

## 264 | 4.2 The pCO<sub>2</sub> estimates results

265

### 266 4.2.1 The regression approach

267 The summary of stomatal parameters of the fossil *Nageia* and reconstruction results  
268 are provided in Tables 6–8. The mean SD and SI values of the adaxial surface are 44.5  
269 mm<sup>-2</sup> and 1.8 %, respectively (Table 6). The mean SD and SI values of the abaxial  
270 surface are 49.8 mm<sup>-2</sup> and 2.07 %, respectively (Table 7).

271 Based on the regression approach, the pCO<sub>2</sub> was reconstructed as 351.9 ± 6.6 ppmv  
272 and 365.6 ± 7.6 ppmv according to the SD of adaxial and abaxial sides. The combined  
273 SD value is an average of 46.6 mm<sup>-2</sup> (Table 8), giving the reconstructed pCO<sub>2</sub> of  
274 358.1 ± 5.0 ppmv.

275

### 276 4.2.2 The stomatal ratio method

277 Mean SR value of the adaxial side (SR=1.69 ± 0.18) is a little larger than that of the  
278 abaxial side (SR=1.60 ± 0.11) in fossil *Nageia* leaves (Tables 6 and 7). The pCO<sub>2</sub>  
279 reconstruction results are 537.5 ± 56.5 ppmv (Table 6) and 496.1 ± 35.7 ppmv (Table 7)  
280 based on the adaxial and abaxial cuticles, respectively. Based on the combined SD of  
281 both leaf sides, the pCO<sub>2</sub> result is 519.9 ± 35.0 ppmv.

282 The partial pressure of CO<sub>2</sub> decreases with elevation (Gale, 1972). Jones (1992)  
283 proposed that the relationship between elevation and partial pressure in the lower  
284 atmosphere can be expressed as  $P = -10.6E + 100$ , where  $E$  is elevation in kilometers  
285 and  $P$  is the percentage of partial pressure relative to sea level. Various studies



286 corroborate that SI and SD of many plants have positive correlations with altitude  
287 (Körner and Cochrane, 1985; Woodward, 1986; Woodward and Bazzaz, 1988;  
288 Beerling et al., 1992; Rundgren and Beerling, 1999) while they are negatively related  
289 to the partial pressure of CO<sub>2</sub> (Woodward and Bazzaz, 1988). Therefore, it is essential  
290 to take elevation calibration into account during pCO<sub>2</sub> concentration estimates.  
291 However, Royer (2003) pointed out that it is unnecessary to provide this conversion  
292 when trees lived at <250 m in elevation. In this paper, the nearest living equivalent  
293 species, *Nageia motleyi*, grows at 5 m in elevation with  $P = 99.9$ , suggesting that CO<sub>2</sub>  
294 concentration estimates were only underestimated by 0.1%. Consequently, no  
295 correction is needed for the reconstruction result in this study. After being projected  
296 into a long-term carbon cycle model (GEOCARB III; Berner and Kothavalá 2001),  
297 the results of this study compares well with CO<sub>2</sub> concentrations for corresponding age  
298 within their error ranges (Fig. 5).

299

## 300 | **5 Discussion**

301

### 302 | **5.1 Stomatal parameters response to CO<sub>2</sub>**

303

304 | ~~For modern *Nageia*. Here,~~ we find that SD decreases as atmospheric CO<sub>2</sub>  
305 | concentrations increase, ~~however, but that~~ SI does not. Generally, SI is more sensitive  
306 | in response to the atmospheric CO<sub>2</sub> concentration than SD (Beerling, 1999; Royer,  
307 | 2001). However, the reverse case ~~has been observed for some flora. is not unfound.~~

308 For example, Kouwenberg et al. (2003) reported that SD is better than SI in reflecting  
309 the negative relationships with CO<sub>2</sub> in conifer needles, accounting for the special  
310 paralleled mode of the ordinary epidermal and stomatal formation. Although *Nageia*  
311 is broad-leaved rather than needle-leaved, it also has well paralleled epidermal cells,  
312 ~~herein showing the different relationships between CO<sub>2</sub> and SD or SI.~~

313 Compared with SD, the SDL has weaker correlation with CO<sub>2</sub> at a smaller R<sup>2</sup>. The  
314 SNL and TSDL have no response to the change of CO<sub>2</sub>. The insensitivity of SNL,  
315 SDL and TSDL might account for the characters of broad-leaved leaf shape and  
316 paralleled epidermal cells. The SNL should be applied to conifer needles with single  
317 file of stomata (Kouwenberg et al., 2003). The SDL and TSDL were considered as the  
318 most appropriate method when the stomatal rows grouped in bands in a hypo- or  
319 amphistomatal conifer needle species (Kouwenberg et al., 2003). Considering all the  
320 stomatal parameters above, SD appears to be the most sensitive to CO<sub>2</sub>.

321 The SD-CO<sub>2</sub> correlation shows one value from leaf No. 40798 offset from the  
322 others. The SI-CO<sub>2</sub> correlation shows different offset values in different leaf sides.  
323 The offset values might be affected by leaf maturity and light intensity. However, it is  
324 hard to distinguish whether a fossil leaf ~~is was~~ young or mature, ~~or grew in a sunny or~~  
325 ~~shady environment~~ ~~live in the sunny or shady light regimes.~~

326 The R<sup>2</sup> value (0.5) of SD-CO<sub>2</sub> based on the adaxial side is higher than from the  
327 abaxial side and the combination of both sides, indicating that the correlation of  
328 SD-CO<sub>2</sub> is stronger than the others parameters herein. Therefore, the SD on the  
329 adaxial side is the best in reconstructing pCO<sub>2</sub>. The reconstruction result based on the

330 regression approach is  $351.9 \pm 6.6$  ppmv lower than the one based on the stomatal  
331 ratio method (Table 6), and it is relatively lower than the results based on the other  
332 proxies (Fig. 6; Freeman and Hayes, 1992; Pagani et al., 2005; Maxbauer et al., 2014).  
333 However, the result based on stomatal ratio method is  $537.5 \pm 56.5$  ppmv, which is  
334 fairly close to GEOCARB III predictions (Fig. 5) and historical reconstruction  
335 trends (Fig. 6).

336

## 337 5.2 Paleoclimate reconstructed history

338

339 The pCO<sub>2</sub> levels throughout the Cenozoic were relatively generally lower than  
340 during much of the Cretaceous, but probably also decreased significantly from  
341 the early to late Eocene. However, there is a wide range of estimates for the Eocene  
342 (Koch et al., 1992; Sinha and Stott, 1994; Ekart et al., 1999; Greenwood et al., 2003;  
343 Royer, 2003; Pagani et al., 2005; Wing et al., 2005; Lowenstein and Demicco, 2006;  
344 Fletcher et al., 2008; Zachos et al., 2008; Beerling et al., 2009; Bijl et al., 2010; Smith  
345 et al., 2010; Doria et al., 2011; Kato et al., 2011; Maxbauer et al., 2014). ~~(Ekart et al.,~~  
346 ~~1999), but had an overall decreasing trend with some significant increases on~~  
347 ~~short time scales (e.g. in the earliest Eocene and middle Miocene, Zachos et al., 2001,~~  
348 ~~2008; Wing et al., 2005; Lowenstein and Demicco, 2006; Fletcher et al., 2008; Bijl et~~  
349 ~~al., 2010; Kato et al., 2011). There is a wide range in pCO<sub>2</sub> estimates for the~~  
350 ~~Paleogene, reflecting problems in the various proxies. Both the fractionation of~~  
351 ~~carbon isotopes by phytoplankton (Freeman and Hayes, 1992) and analysis of~~

352 ~~paleosol (fossil soil) carbonates (Ekart et al., 1999) demonstrate that carbon dioxide-~~  
353 ~~levels were less than 1000 ppmv before the Cretaceous-Tertiary boundary and have-~~  
354 ~~been decreasing since the Paleocene.~~  
355 ~~Based on the measurements of palaeosol carbon isotopes, Cerling (1991) reported that~~  
356 ~~pCO<sub>2</sub> levels for the Eocene and Miocene through to the present was lower than 700-~~  
357 ~~ppmv. Fletcher et al. (2008) also showed that atmospheric CO<sub>2</sub> levels were~~  
358 ~~approximately 680 ppmv by 60 million years ago. However, Stott (1992)~~  
359 ~~reconstructed pCO<sub>2</sub> as 450–550 ppmv for the early Eocene based on phytoplankton-~~  
360 ~~Additionally, reconstructions using the stomatal ratio method based on *Ginkgo*,~~  
361 ~~*Metasequoia*, and Lauraceae leaves also revealed a low pCO<sub>2</sub> level between 300 and~~  
362 ~~500 ppmv during the early Eocene (Kürschner et al., 2001; Royer et al., 2001;~~  
363 ~~Greenwood et al., 2003; Royer, 2003) except a single high estimate of about 800-~~  
364 ~~ppmv near the Paleocene/Eocene boundary (Royer et al., 2001).~~  
365 ~~Subsequently,~~ Smith et al. (2010) reconstructed the value of the early Eocene pCO<sub>2</sub>  
366 ranging from 580 ± 40 to 780 ± 50 ppmv using the stomatal ratio method (recent  
367 standardization) based on both SI and SD. A climatic optimum occurred in the middle  
368 Eocene (MECO); the reconstructed CO<sub>2</sub> concentrations are mainly between 700 ~~and-~~  
369 to 1000 ppmv during the late middle Eocene climate transition (42–38 Ma) using  
370 stomatal indices of fossil *Metasequoia* needles, but concentrations declined to 450  
371 ppmv toward the top of the investigated section (Doria et al., 2011). Jacques et al.  
372 (2014) used CLAMP to calibrate climate change in Antarctica during the early-middle  
373 Eocene, suggesting a seasonal alternation of high- and low-pressure systems over

带格式的: 缩进: 首行缩进: 0 厘米

带格式的: 首行缩进: 1 字符

374 Antarctica during the early-middle Eocene. Spicer et al. (2014) also reconstructed a  
375 relatively lower cool temperature than  $\delta^{18}\text{O}$  records (Keating-Bitonti et al., 2011) in  
376 the middle Eocene of Hainan Island, South China using CLAMP, indicating a not  
377 uniformly warm climate in the low latitude during the Eocene. An overall decreasing  
378 trend of the  $\text{pCO}_2$  level was presented after the middle Eocene (Fig. 6; Retallack,  
379 2009b).

380 The ice-sheets started to appear in the Antarctic during the Late Eocene (Zachos et  
381 al., 2001), then the temperature suffered an apparent further decrease from the late  
382 Eocene ~~to the early Oligocene onwards (Fig. 6). (Roth-Nebelsiek et al., 2004), which~~  
383 ~~resulted in the Antarctic being almost fully covered by ice sheets. Subsequently, the~~  
384 ~~climate variation was comparatively stable with a little wobbling in temperature~~  
385 ~~during the Oligocene period (Fig. 6), while a small and ephemeral Late Oligocene~~  
386 ~~Warming was present in the latest part of the Oligocene, resulting in reducing the~~  
387 ~~Antarctic ice sheets to a minimum and forming a brief period of glaciation at that time~~  
388 ~~(Zachos et al., 2001). During the Middle Miocene, a quick rise in temperature was~~  
389 ~~shown, which was followed by a small glaciation (Fig. 6; Zachos et al., 2001;~~  
390 ~~Roth-Nebelsiek et al., 2004; Beerling and Royer, 2011). Subsequently, the  $\text{CO}_2$~~   
391 ~~concentration decreased gradually and reached 280 ppmv until the period of the~~  
392 ~~industrial revolution (Fig. 6). Since then, however, the  $\text{CO}_2$  concentration rebounded~~  
393 ~~to present day level.~~

394

395 In conclusion, although various results were made by different  $\text{pCO}_2$  reconstruction

396 proxies at the same time, their entire decreasing tendency of pCO<sub>2</sub> level are  
397 remarkably consistent with each other since the Eocene (Fig. 6). Fig. 6 shows that  
398 during the Eocene the temperature was higher than at present. Comparing to the  
399 estimates of late middle Eocene pCO<sub>2</sub> by Doria et al. (2011), the present result~~The~~  
400 ~~reconstructed pCO<sub>2</sub> of 351.9 ± 6.6 ppmv based on the regression approach is~~ shows a  
401 remarkably lower pCO<sub>2</sub> level, ~~during the early late Eocene. The result while the one~~  
402 based on the stomatal ratio method of 537.5 ± 56.5 ppmv is within the variation range  
403 of 500–1000 ppmv, which is closely consistent with the pCO<sub>2</sub> changes over the  
404 geological ages (Fig. 6). The world was dynamic in the Paleogene, including in the  
405 late middle Eocene, when the MECO occurred. Thus, the exact age matters, and it is  
406 possible that the values may differ because of slight offsets in time.

带格式的: 缩进: 首行缩进: 0.42 厘米

带格式的: 缩进: 首行缩进: 0 厘米

## 410 6 Conclusion

411  
412 In this study, we reconstructed ~~the~~ late middle Eocene pCO<sub>2</sub> based on the fossil  
413 leaves of *Nageia maomingensis* Jin et Liu from ~~the~~ late middle Eocene of Maoming  
414 Basin, Guangdong Province, China. *Nageia* is a special element in conifers by its  
415 broad multi-veined leaf that lacks mid-vein. The stomatal data analysis suggests that  
416 only stomatal densities (SD) from both sides of *Nageia motleyi* leaves have significant  
417 negative correlations with the atmospheric CO<sub>2</sub> concentration. The SD from the

418 adaxial side gives the best correlation to the CO<sub>2</sub>. Based on SDs, the pCO<sub>2</sub>  
419 concentration is reconstructed using both the regression approach and the stomatal  
420 ratio method. The pCO<sub>2</sub> result based on the regression approach is 351.9 ± 6.6 ppmv,  
421 showing a relatively lower CO<sub>2</sub> level. The reconstructed result based on the stomatal  
422 ratio method is 537.5 ± 56.5 ppmv consistent with the variation trends based on the  
423 other proxies. Here, we explored the potential of *N. maomingensis* in pCO<sub>2</sub>  
424 reconstruction and obtained different results according to different methods, providing  
425 a new insight for the reconstruction of paleoclimate and paleoenvironment in conifers.

426  
427 *Acknowledgements.* This study was supported by the National Natural Science  
428 Foundation of China (Grant No. 41210001, 41572011), and the Fundamental  
429 Research Funds for the Central Universities ~~(Grant No. 121gjc04), and the Key Project~~  
430 ~~of Sun Yat-sen University for inviting foreign teachers.~~ We greatly thank the  
431 Herbarium of the V.L. Komarov Botanical Institute of the Russian Academy of  
432 Sciences (LE) for the permission to examine and collect extant *Nageia* specimens. We  
433 also express sincere gratitude to Prof. Sun Tongxing (Yancheng Teachers University),  
434 Dr. David Boufford (Harvard University) and Dr. Richard Chung Cheng Kong (Forest  
435 Research Institute Malaysia) for providing extant *N. motleyi* leaves from the  
436 herbarium of the Royal Botanic Garden at Edinburgh (E), the Harvard University  
437 Herbaria (A/GH) and the herbarium of Forest Research Institute Malaysia (KEP). We  
438 sincerely appreciate the guidance of Chengqian Wang (Harbin Institute of Technology)  
439 on preparing Figs. 3–6. We also offer sincere gratitude to Prof. Steven R. Manchester

440 and Mr. Terry Lott (Florida Museum of Natural History, University of Florida) for  
441 suggestions and modification.



442 **References**

- 443 Bai, Y. J., Chen, L. Q., Ranhotra, S. P., Wang, Q., Wang, Y. F., Li, C. S.:  
444 Reconstructing atmospheric CO<sub>2</sub> during the Plio–Pleistocene transition by fossil  
445 *Typha*. *Global Change Biology*, 21, 874–881, doi:10.1111/gcb.12670, 2015.
- 446 Beerling, D. J.: Stomatal density and index: theory and application, in: Jones, T. P.,  
447 and Rowe, N. P., (Eds.), *Fossil Plants and Spores: Modern Techniques*,  
448 Geological Society, London, 251–256, 1999.
- 449 Beerling, D. J., and Kelly, C. K.: Stomatal density responses of temperate woodland  
450 plants over the past seven decades of CO<sub>2</sub> increase: A comparison of salisbury  
451 (1927) with contemporary data, *American Journal of Botany*, 84, 1572–1583,  
452 1997.
- 453 Beerling, D. J., and Royer, D. L.: Reading a CO<sub>2</sub> signal from fossil stomata, *New*  
454 *Phytologist*, 153, 387–397, doi:10.1046/j.0028-646X.2001.00335.x, 2002.
- 455 Beerling, D. J., and Royer, D. L.: Convergent Cenozoic CO<sub>2</sub> history, *Natural*  
456 *Geoscience*, 4, 418–420, doi:10.1038/ngeo1186, 2011.
- 457 Beerling, D. J., Chaloner, W. G., Huntley, B., Pearson, J. A., Tooley, M. J., and  
458 Woodward, F. I.: Variations in the stomatal density of *Salix herbacea* L. under  
459 the changing atmospheric CO<sub>2</sub> concentrations of late- and post-glacial time,  
460 *Philosophical Transactions of the Royal Society of London*, ser. B. 336, 215–224,  
461 doi:10.1098/rstb.1992.0057, 1992.
- 462 Beerling, D. J., Fox, A., and Anderson, C. W.: Quantitative uncertainty analyses of  
463 ancient atmospheric CO<sub>2</sub> estimates from fossil leaves, *American Journal of*

464 Science, 309, 775–787, doi:10.2475/09.2009.01, 2009.

465 Beerling, D. J., Lomax, B. H., Royer, D. L., Upchurch Jr., G. R., and Kump, L. R.: An  
466 atmospheric  $p\text{CO}_2$  reconstruction across the Cretaceous-Tertiary boundary from  
467 leaf megafossils, Proceedings of the National Academy of Sciences of the United  
468 States of America, 99, 7836–7840, doi:10.1073/pnas.122573099, 2002.

469 Berner, R. A.: GEOCARB II: A revised model of atmospheric  $\text{CO}_2$  over Phanerozoic  
470 time, American Journal of Science, 294, 56–91, doi:10.2475/ajs.294.1.56, 1994.

471 Berner, R. A., and Kothaval á Z.: GEOCARB III: A revised model of Atmospheric  
472  $\text{CO}_2$  over Phanerozoic time, American Journal of Science, 301, 182–204,  
473 doi:10.2475/ajs.301.2.182, 2001.

474 Bijl, P. K., Houben, A. J. P., Schouten, S., Bohaty, S. M., Sluijs, A., Reichart, G.,  
475 Sinninghe Damst é J. S., and Brinkhuis, H.: Transient Middle Eocene  
476 atmospheric  $\text{CO}_2$  and temperature variations, Science, 330, 819–821,  
477 doi:10.1126/science.1193654, 2010.

478 Brown, L. R.: Atmospheric carbon dioxide concentration, 1000-2009 (Supporting  
479 data), in: Brown, L. R., (Ed.), World on the Edge: How to Prevent Environmental  
480 and Economic Collapse. Chapter 4 Data: Rising Temperatures, Melting Ice, and  
481 Food Security, Earth policy institute, Norton, W.W. & Company, New York,  
482 London ([http://www.earth-policy.org/books/wote/wote\\_data](http://www.earth-policy.org/books/wote/wote_data)), 2010.

483 ~~Cerling, T. E.: Carbon dioxide in the atmosphere: evidence from Cenozoic and~~  
484 ~~Mesozoic palaeosols, American Journal of Science, 291, 377–400,~~  
485 ~~doi:10.2475/ajs.291.4.377, 1991.~~

486 Cerling, T. E.: Use of carbon isotopes in paleosols as an indicator of the P(CO<sub>2</sub>) of the  
487 paleoatmosphere, *Global Biogeochemical Cycles*, 6, 307–314,  
488 doi:10.1029/92GB01102, 1992.

489 Chaloner, W. G., and McElwain, J. C.: The fossil plant record and global climate  
490 change, *Review of Palaeobotany and Palynology*, 95, 73–82,  
491 doi:10.1016/S0034-6667(96)00028-0, 1997.

492 Cheng, W. C., Fu, L. K., and Chao, C. S.: *Podocarpus* (Podocarpaceae), in: Cheng,  
493 Wanch ün, and Fu, Likuo, (Eds.), *Flora of China*, Science Press, Beijing, 7,  
494 398–422, 1978 (in Chinese).

495 Doria, G., Royer, D. L., Wolfe, A. P., Fox, A., Westgate, J. A., and Beerling, D. J.:  
496 Declining atmospheric CO<sub>2</sub> during the Late Middle Eocene climate transition,  
497 *American Journal of Science*, 311, 63–75, doi:10.2475/01.2011.03, 2011.

498 Ekart, D. D., Cerling, T. E., Montanez, I. P., and Tabor, N. J.: A 400 million year  
499 carbon isotope record of pedogenic carbonate: implications for paleoatmospheric  
500 carbon dioxide, *American Journal of Science*, 299, 805–827,  
501 doi:10.2475/ajs.299.10.805, 1999.

502 Fletcher, B. J., Brentnall, S. J., Anderson, C. W., Berner, R. A., and Beerling, D. J.:  
503 Atmospheric carbon dioxide linked with Mesozoic and Early Cenozoic climate  
504 change, *Nature Geoscience*, 1, 43–48, doi:10.1038/ngeo.2007.29, 2008.

505 Freeman, K. H., and Hayes, J. M.: Fractionation of carbon isotopes by phytoplankton  
506 and estimates of ancient CO<sub>2</sub> levels, *Global Biogeochemical Cycles*, 6, 185–198,  
507 doi:10.1029/92GB00190, 1992.

508 Fu, D. Z.: Nageiaceae – a new gymnosperm family, *Acta Phytotaxonomica Sinica*, 30,  
509 515–528, 1992 (in Chinese with English summary).

510 Fu L. K., Li Y., and Mill, R. R.: Podocarpaceae, in: Wu Z. Y., and Raven, P. H., (Eds.),  
511 Flora of China, Science Press, Beijing, 4, 78–84, 1999.

512 Gale, J.: Availability of carbon dioxide for photosynthesis at high altitudes: theoretical  
513 considerations, *Ecology*, 53, 494–497, doi:10.2307/1934239, 1972.

514 Greenwood, D. G., Scarr, M. J., and Christophel, D. C.: Leaf stomatal frequency in the  
515 Australian tropical rain forest tree *Neolitseadealbata* (Lauraceae) as a proxy  
516 measure of atmospheric  $p\text{CO}_2$ , *Palaeogeography, Palaeoclimatology,*  
517 *Palaeoecology*, 196, 375–393, doi:10.1016/S0031-0182(03)00465-6, 2003.

518 Grein, M., Oehm, C., Konrad, W., Utescher, T., Kunzmann, L., and Roth-Nebelsick,  
519 A.: Atmospheric  $\text{CO}_2$  from the late Oligocene to early Miocene based on  
520 photosynthesis data and fossil leaf characteristics, *Palaeogeography,*  
521 *Palaeoclimatology, Palaeoecology*, 374, 41–51,  
522 doi:10.1016/j.palaeo.2012.12.025, 2013.

523 Henderiks, J., and Pagani, M.: Coccolithophore cell size and the Paleogene decline in  
524 atmospheric  $\text{CO}_2$ , *Earth and Planetary Science Letters* 269, 575–583,  
525 doi:10.1016/j.epsl.2008.03.016, 2008.

526 Hill, R. S., and Pole, M. S.: Leaf and shoot morphology of extant *Afrocarpus*, *Nageia*  
527 and *Retrophyllum* (Podocarpaceae) species, and species with similar leaf  
528 arrangement, from Tertiary sediments in Australasia, *Australian Systematic*  
529 *Botany*, 5, 337–358, doi:10.1071/SB9920337, 1992.

530 Hu, J. J., Xing, Y. W., Turkington, R., Jacques, F. M. B. Su, T., Huang, Y. J. and Zhou  
531 Z. K.: A new positive relationship between pCO<sub>2</sub> and stomatal frequency in  
532 *Quercus guyavifolia* (Fagaceae): a potential proxy for palaeo-CO<sub>2</sub> levels, *Annals*  
533 *of Botany*, 1–12, doi:10.1093/aob/mcv007, 2015.

534 Huang, C., Retallack, G. J., Wang, C., and Huang, Q.: Paleatmospheric pCO<sub>2</sub>  
535 fluctuations across the Cretaceous-Tertiary boundary recorded from paleosol  
536 carbonates in NE China, *Palaeogeography, Palaeoclimatology, Palaeoecology*,  
537 385, 95–105, doi.org/10.1016/j.palaeo.2013.01.005, 2013.

538 Jacques, F. M. B., Shi, G. L., Li, H. M., and Wang, W. M.: An Early-Middle Eocene  
539 Antarctic summer monsoon: Evidence of ‘fossil climates’, *Gondwana Research*,  
540 25, 1422–1428, doi:10.1016/j.gr.2012.08.007, 2014.

541 Jin, J. H., Qiu, J., Zhu, Y. A., and Kodrul, T. M.: First fossil record of the genus  
542 *Nageia* (Podocarpaceae) in South China and its phytogeographic implications,  
543 *Plant Systematics and Evolution*, 285, 159–163, doi:10.1007/s00606-010-0267-4,  
544 2010.

545 Jones, H. G.: *Plants and microclimate*, Cambridge UK Cambridge University Press,  
546 1–428, 1992.

547 Kato, Y., Fujinaga, K., and Suzuki, K.: Marine Os isotopic fluctuations in the Early  
548 Eocene greenhouse interval as recorded by metalliferous umbers from a Tertiary  
549 ophiolite in Japan, *Gondwana Research*, 20, 594–607,  
550 doi:10.1016/j.gr.2010.12.007, 2011.

551 Keating-Bitonti, C. R., Ivany, L. C., Affek, H. P., Douglas, P., and Samson, S. D.:

552 Warm, not super-hot, temperatures in the early Eocene subtropics, *Geology* 39,  
553 771–774, doi: 10.1130/G32054.1, 2011.

554 Kimura, T., Ohana, T., and Mimoto, K.: Discovery of a podocarpaceous plant from  
555 the Lower Cretaceous of Kochi Prefecture, in the outer zone of southwest Japan,  
556 *Proceedings of the Japan Academy, ser. B*, 64, 213–216, doi:10.2183/pjab.64.213,  
557 1988.

558 Koch, P. L., Zachos, J. C., and Gingerich, P. D.: Correlation between isotope records  
559 in marine and continental carbon reservoirs near the Palaeocene/Eocene  
560 boundary, *Nature*, 358, 319–322, doi:10.1038/358319a0, 1992.

561 Kouwenberg, L. L. R., McElwain J. C., Kürschner, W. M., Wagner, F., Beerling, S. J.,  
562 Mayle, F. E., and Visscher, H.: stomatal frequency adjustment of four conifer  
563 species to historical changes in atmospheric CO<sub>2</sub>, *American Journal of Botany*,  
564 90, 610–619, 2003.

565 Körner, Ch., and Cochrane, P. M.: Stomatal responses and water relations of  
566 *Eucalyptus pauciflora* in summer along an elevational gradient, *Oecologia*, 66,  
567 443–455, doi:10.1007/BF00378313, 1985.

568 Krassilov, V. A.: New coniferales from Lower Cretaceous of Primorye, *Botanical*  
569 *Journal*, 50, 1450–1455 (in Russia), 1965.

570 Kürschner, W. M., van der Burgh, J., Visscher, H., and Dilcher, D. L.: Oak leaves as  
571 biosensors of Late Neogene and Early Pleistocene paleoatmospheric CO<sub>2</sub>  
572 concentrations, *Marine Micropaleontology*, 27, 299–312,  
573 doi:10.1016/0377-8398(95)00067-4, 1996.

574 Kürschner, W. M., Wagner, F., Dilcher, D. L., and Visscher, H.: Using fossil leaves for  
575 the reconstruction of Cenozoic paleoatmospheric CO<sub>2</sub> concentrations, in:  
576 Gerhard, L. C., Harrison, W. E., Hanson, B. M., (Eds.), Geological Perspectives  
577 of Global Climate Change, APPG Studies in Geology, 47, Tulsa, 169–189, 2001.

578 Kürschner, W. M., Kvaček, Z., and Dilcher, D. L.: The impact of Miocene  
579 atmospheric carbon dioxide fluctuations on climate and the evolution of  
580 terrestrial ecosystems, Proceedings of the National Academy of Sciences of the  
581 United States of America, 105, 449–453, doi:10.1073/pnas.0708588105, 2008.

582 Liu, X. Y., Gao, Q., and Jin, J. H.: Late Eocene leaves of *Nageia* Gaertner (section  
583 *Dammaroideae* Mill) from Maoming Basin, South China and their implications  
584 on phytogeography, Journal of Systematics and Evolution, 53, 297–307,  
585 doi:10.1111/jse.12133, 2015.

586 Lowenstein, T. K., and Demicco, R. V.: Elevated Eocene atmospheric CO<sub>2</sub> and its  
587 subsequent decline, Science, 313, 1928, doi:10.1126/science.1129555, 2006.

588 McElwain, J. C.: Do fossil plants signal palaeoatmospheric carbon dioxide  
589 concentration in the geological past, Philosophical Transactions of the Royal  
590 Society, Lond B, 353, 83–96, doi:10.1098/rstb.1998.0193, 1998.

591 McElwain, J. C., and Chaloner, W. G.: Stomatal density and index of fossil plants  
592 track atmospheric carbon dioxide in the Palaeozoic, Annals of Botany, 76,  
593 389–395, doi:10.1006/anbo.1995.1112, 1995.

594 McElwain, J. C., and Chaloner, W. G.: The fossil cuticle as a skeletal record of  
595 environmental changes, Palaios, 11, 376–388, doi: 10.2307/3515247, 1996.

596 Mill, R. R.: A new combination in *Nageia* (Podocarpaceae): *Novon*, 9, 77–78, 1999.

597 Mill, R. R.: A new sectional combination in *Nageia* Gaertn (Podocarpaceae),  
598 *Edinburgh Journal of Botany*, 58, 499–501, doi:10.1017/S0960428601000804,  
599 2001.

600 Maxbauer, D. P., Royer, D. L., and LePage, B. A.: High Arctic forests during the  
601 middle Eocene supported by moderate levels of atmospheric CO<sub>2</sub>, *Geology*, 42,  
602 1027–1030, doi:10.1130/G36014.1, 2014.

603 Moran, K., Backman, J., Brinkhuis, H., Clemens, S. C., Cronin, T., Dickens, G. R.,  
604 Eynaud, F., Gattacceca, J., Jakobsson, M., Jordan, R. W., Kaminski, M., King, J.,  
605 Koc, N., Krylov, A., Martinez, N., Matthiessen, J., McInroy, D., Moore, T.C.,  
606 Onodera, J., O'Regan, M., Päike, H., Rea, B., Rio, D., Sakamoto, T., Smith, D.  
607 C., Stein, R., St John, K., Suto, I., Suzuki, N., Takahashi, K., Watanabe, M.,  
608 Yamamoto, M., Farrell, J., Frank, M., Kubik, P., Jokat, W., and Kristoffersen, Y.:  
609 The Cenozoic palaeoenvironment of the Arctic Ocean, *Nature*, 441, 601–605,  
610 doi:10.1038/nature04800, 2006.

611 Nordt, L., Atchley, S., and Dworkin, S. I.: Paleosol barometer indicates extreme  
612 fluctuations in atmospheric CO<sub>2</sub> across the Cretaceous-Tertiary boundary,  
613 *Geology*, 30, 703–706, doi:10.1130/0091-7613(2002)030<0703:PBIEFI>  
614 2.0.CO;2, 2002.

615 Pagani, M., Arthur, M. A., and Freeman, K. H.: Miocene evolution of atmospheric  
616 carbon dioxide, *Paleoceanography*, 14, doi:10.1029/1999PA900006, 273–292,  
617 1999.



618 Pagani, M., Zachos, J. C., Freeman, K. H., Tipple, B., and Bohaty, S.: Marked decline  
619 in atmospheric carbon dioxide concentrations during the Paleocene, *Science*, 309,  
620 600–603, doi:10.1126/science.1110063, 2005.

621 Pearson, P. N., Foster, G. L., and Wade, B. S.: Atmospheric carbon dioxide through the  
622 Eocene-Oligocene climate transition, *Nature*, 461, 1110–1113,  
623 doi:10.1038/nature08447, 2009.

624 Petit, J. R., Jouzel, J., Raynaud, D., Barkov, N. I., Barnola, J.-M., Basile, I., Bender,  
625 M., Chappellaz, J., Davis, M., Delaygue, G., Delmotte, M., Kotlyakov, V. M.,  
626 Legrand, M., Lipenkov, V. Y., Lorius, C., Pépin, L., Ritz, C., Saltzman, E., and  
627 Stievenard, M.: Climate and atmospheric history of the past 420,000 years from  
628 the Vostok ice core, Antarctica, *Nature*, 399, 429–436, doi:10.1038/20859, 1999.

629 Pieter, T., and Keeling, R.: Recent monthly average Mauna Loa CO<sub>2</sub>, NOAA/ESRL,  
630 [www.esrl.noaa.gov/gmd/ccgg/trends/](http://www.esrl.noaa.gov/gmd/ccgg/trends/) (accessed March 2015), 2015.

631 Poole, I., and Kürschner, W. M.: Stomatal density and index: the practice, in: Jones,  
632 T.P., and Rowe, N.P., (Eds.), *Fossil Plants and Spores: Modern Techniques*,  
633 Geological Society, London, 257–260, 1999.

634 Retallack, G. J.: A 300-million-year record of atmospheric carbon dioxide from fossil  
635 plant cuticles, *Nature*, 411, 287–290, doi:10.1038/35077041, 2001.

636 Retallack, G. J.: Greenhouse crises of the past 300 million years, *Geological Society*  
637 *of America Bulletin*, 121, 1441–1455, doi:10.1130/B26341.1, 2009a.

638 Retallack, G. J.: Refining a pedogenic-carbonate CO<sub>2</sub> paleobarometer to quantify a  
639 Middle Miocene greenhouse spike, *Palaeogeography, Palaeoclimatology,*

640 Palaeoecology, 281, 57–65, doi:10.1016/j.palaeo.2009.07.011, 2009b.

641 ~~Roth-Nebelsick, A., Utescher, T., Mosbrugger, V., Diester-Haass, L., and Walther, H.:~~  
642 ~~Changes in atmospheric CO<sub>2</sub> concentrations and climate from the Late Eocene to~~  
643 ~~Early Miocene: palaeobotanical reconstruction based on fossil floras from~~  
644 ~~Saxony, Germany, Palaeogeography, Palaeoclimatology, Palaeoecology, 205,~~  
645 ~~43–67, doi:10.1016/j.palaeo.2003.11.014, 2004.~~

646 Roth-Nebelsick, A., Grein, M., Utescher, T., and Konrad, W.: Stomatal pore length  
647 change in leaves of *Eotrigonobalanus furcinervis* (Fagaceae) from the Late  
648 Eocene to the Latest Oligocene and its impact on gas exchange and CO<sub>2</sub>  
649 reconstruction, Review of Palaeobotany and Palynology, 174, 106–112,  
650 doi:10.1016/j.revpalbo.2012.01.001, 2012.

651 Roth-Nebelsick, A., Oehm, C., Grein, M., Utescher, T., Kunzmann, L., Friedrich, J.-P.,  
652 and Konrad, W.: Stomatal density and index data of *Platanus neptuni* leaf fossils  
653 and their evaluation as a CO<sub>2</sub> proxy for the Oligocene, Review of Palaeobotany  
654 and Palynology, 206, 1–9, doi:10.1016/j.revpalbo.2014.03.001, 2014.

655 Royer, D. L.: Stomatal density and stomatal index as indicators of paleoatmospheric  
656 CO<sub>2</sub> concentration, Review of Palaeobotany and Palynology, 114, 1–28,  
657 doi:10.1016/S0034-6667(00)00074-9, 2001.

658 Royer, D. L.: Estimating Latest Cretaceous and Tertiary atmospheric CO<sub>2</sub> from  
659 stomatal indices, in: Wing, S. L., Gingerich, P. D., Schmitz, B., and Thomas, E.,  
660 (Eds.), Causes and Consequences of Globally Warm Climates in the Early  
661 Paleocene, Geological Society of America Special Paper, 79–93, 2003.

662 Royer, D. L.: CO<sub>2</sub>-forced climate thresholds during the Phanerozoic, *Geochimica et*  
663 *Cosmochimica Acta*, 70, 5665–5675, doi:10.1016/j.gca.2005.11.031, 2006.

664 Royer, D. L., Wing, S. L., Beerling, D. J., Jolley, D. W., Koch, P. L., Hickey, L. J., and  
665 Berner, R. A.: Paleobotanical evidence for near present-day levels of atmospheric  
666 CO<sub>2</sub> during part of the Tertiary, *Science*, 292, 2310–2313,  
667 doi:10.1126/science.292.5525.2310, 2001.

668 Rundgren, M., and Beerling, D. J.: A Holocene CO<sub>2</sub> record from the stomatal index of  
669 subfossil *Salix herbacea* L. leaves from northern Sweden, *The Holocene*, 9,  
670 509–513, doi:10.1191/095968399677717287, 1999.

671 Seki, O, Foster, G. L., Schmidt, D. N., Mackensen, A., Kawamura, K., and Pancost, R.  
672 D.: Alkenone and boron-based Pliocene *p*CO<sub>2</sub> records, *Earth and Planetary*  
673 *Science Letters*, 292, 201–211, doi:10.1016/j.epsl.2010.01.037, 2010.

674 Sinha, A., and Stott, L. D.: New atmospheric *p*CO<sub>2</sub> estimates from paleosols during  
675 the late Paleocene/early Eocene global warming interval, *Global and Planetary*  
676 *Change*, 9, 297–307, doi:10.1016/0921-8181(94)00010-7, 1994,

677 Smith, R. Y., Greenwood, D. R., and Basinger, J.F.: Estimating paleoatmospheric  
678 *p*CO<sub>2</sub> during the Early Eocene Climatic Optimum from stomatal frequency of  
679 *Ginkgo*, Okanagan Highlands, British Columbia, Canada, *Palaeogeography,*  
680 *Palaeoclimatology, Palaeoecology*, 293, 120–131,  
681 doi:10.1016/j.palaeo.2010.05.006, 2010.

682 Spicer, A. R., Herman, A. B., Liao, W. B., Spicer, T. E. V., Kodrul, T. M., Yang, J., and  
683 Jin, J. H.: Cool tropics in the middle Eocene: Evidence from the Changchang

684 Flora, Hainan Island, China, *Palaeogeography, Palaeoclimatology, Palaeoecology*,  
685 412, 1–16, doi:10.1016/j.palaeo.2014.07.011, 2014.

686 Stott, L. D.: Higher temperatures and lower oceanic  $p\text{CO}_2$ : A climate enigma at the  
687 end of the Paleocene Epoch, *Paleoceanography*, 7, 395–404,  
688 doi:10.1029/92PA01183, 1992.

689 Stults, D. Z., Wagner-Cremer, F., and Axsmith, B. J.: Atmospheric paleo- $\text{CO}_2$   
690 estimates based on *Taxodium distichum* (Cupressaceae) fossils from the Miocene  
691 and Pliocene of Eastern North America, *Palaeogeography Palaeoclimatology*  
692 *Palaeoecology*, 309, 327–332, doi:10.1016/j.palaeo.2011.06.017, 2011.

693 Sun, B. N., Ding, S. T., Wu, J. Y., Dong, C., Xie, S. P., and Lin, Z. C.: Carbon isotope  
694 and stomatal data of Late Pliocene Betulaceae leaves from SW China:  
695 Implications for palaeoatmospheric  $\text{CO}_2$ -levels, *Turkish Journal of Earth*  
696 *Sciences*, 21, 237–250, doi:10.3906/yer-1003-42, 2012.

697 Sun, T. X.: Cuticle micromorphology of *Nageia*, *Journal of Wuhan Botanical*  
698 *Research*, 26, 554–560, doi:10.3969/j.issn.2095-0837.2008.06.002, 2008 (in  
699 Chinese with English abstract).

700 Tripathi, A. K., Roberts, C. D., and Eagle, R. A.: Coupling of  $\text{CO}_2$  and ice sheet  
701 stability over major climate transitions of the last 20 million years, *Science*, 326,  
702 1394–1397, doi:10.1126/science.1178296, 2009.

703 Van der Burgh, J., Visscher, H., Dilcher, D. L., and Kürschner, W. M.:  
704 Paleoatmospheric signatures in Neogene fossil leaves, *Science*, 260, 1788–1790,  
705 doi:10.1126/science.260.5115.1788, 1993.

706 Wang, J. D., Li, H. M., and Zhu Z. Y.: Magnetostratigraphy of Tertiary rocks from  
707 Maoming Basin, Guangdong province, China, Chinese Journal of Geochemistry,  
708 13, 165–175, doi:10.1007/BF02838516, 1994.

709 [Walker, J. D., and Geissman, J. W.: Geologic Time Scale, Geological Society of](#)  
710 [America, doi:10.1130/2009.CTS004R2C, 2009.](#)

711 Wing, S. L., Harrington, G. J., Smith, F. A., Bloch, J. I., Boyer, D. M., and Freeman, K.  
712 H.: Transient floral change and rapid global warming at the Paleocene-Eocene  
713 boundary, Science, 310, 993–996, doi:10.1126/science.1116913, 2005.

714 Woodward, F. I.: Ecophysiological studies on the shrub *Vaccinium myrtillus* L. taken  
715 from a wide altitudinal range, Oecologia, 70, 580–586, doi:10.1007/BF00379908,  
716 1986.

717 Woodward, F. I.: Stomatal numbers are sensitive to increases in CO<sub>2</sub> concentration  
718 from pre-industrial levels, Nature, 327, 617–618, doi:10.1038/327617a0, 1987.

719 Woodward, F. I., and Bazzaz, F. A.: The responses of stomatal density to CO<sub>2</sub> partial  
720 pressure, Journal of Experimental Botany, 39, 1771–1781,  
721 doi:10.1093/jxb/39.12.1771, 1988.

722 Yang, J. J., Qi, G. F., and Xu, R. H.: Studies on fossil woods excavated from the Dabie  
723 mountains, Scientia Silvae Sinicae, 26, 379–386, 1990 (in Chinese with English  
724 abstract).

725 Ye, M. N.: On the preparation methods of fossil cuticle. Palaeontological Society of  
726 China (Ed.), Selected papers of the 12th Annual conference of the  
727 Palaeontological Society of China, Science Press, Beijing, 170–179, 1981 (in

728 Chinese).

729 Zachos, J., Pagani, M., Sloan, L., Thomas, E., and Billups, K.: Trends, rhythms,  
730 aberrations in global climate 65 Ma to present, *Science*, 292, 686–693,  
731 doi:10.1126/science.1059412, 2001.

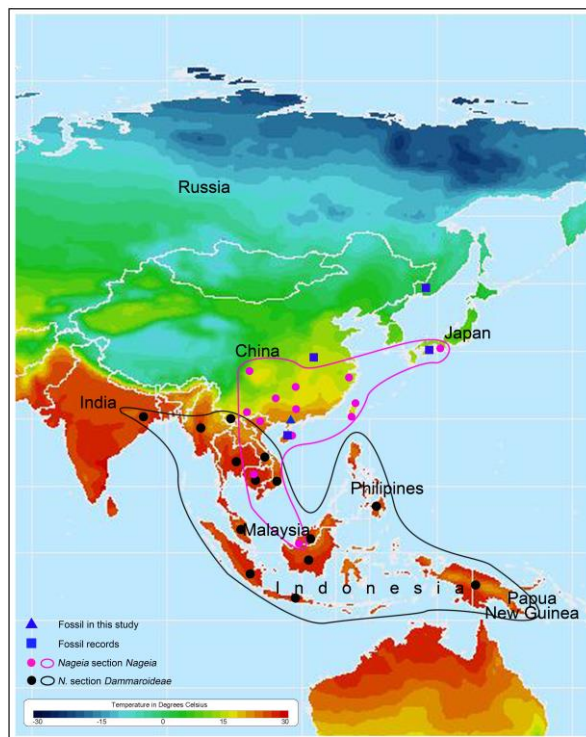
732 Zachos, J., Dickens, G. R. and Zeebe, R. E.: An early Cenozoic perspective on  
733 greenhouse warming and carbon-cycle dynamics, *Nature*, 451, 279–283,  
734 doi:10.1038/nature06588, 2008.

735

736 Figure 1. Map showing the distribution of extant and fossil *Nageia* and their mean annual

737 temperature (Modified after the map from

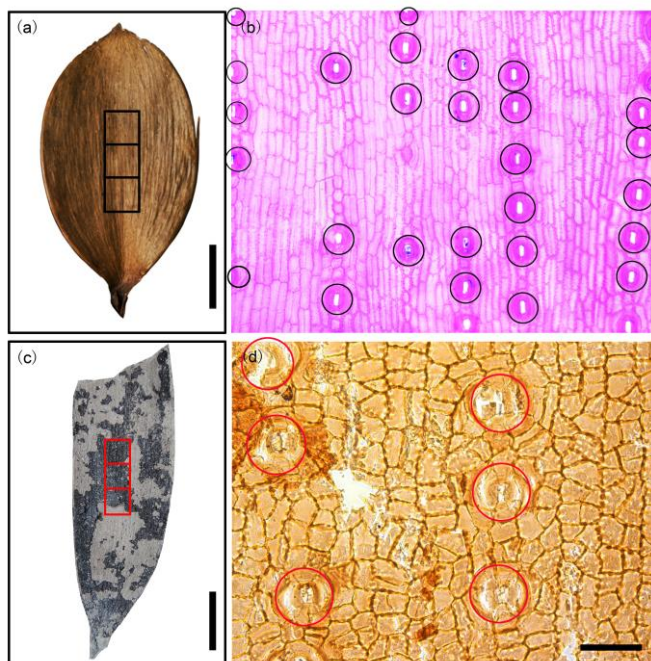
738 <http://www.sage.wisc.edu/atlas/maps.php?datasetid=35&includerelatedlinks=1&dataset=35>).



739

740

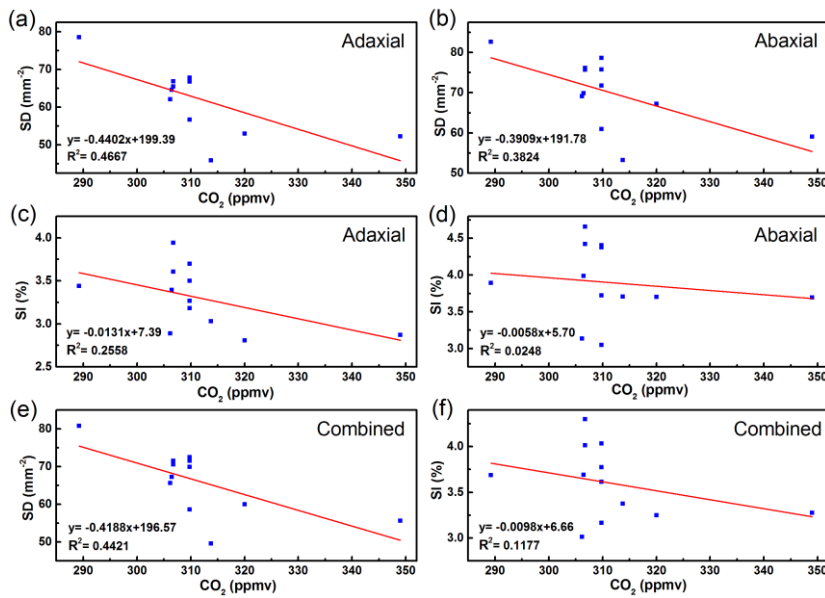
741 Figure 2. Sampling areas and counting rules are shown. (a) *Nageia motleyi* (Parl.) De Laub.leaf.  
742 Black squares in the middle of the leaf show the sampling areas for preparing the cuticles. (b) The  
743 abaxial side of the cuticle from *N. motleyi* leaf. Black circles show the counted stomatal  
744 complexes. (c) *N. maomingensis* Jin et Liu. Red squares in the middle of the leaf indicate the  
745 sampling areas. (d) The abaxial side of the fossil cuticle. Red circles show the counted stomatal  
746 complexes. Scale bars: (a) and (c) = 1 cm; (b) and (d) = 50  $\mu$ m.



747  
748

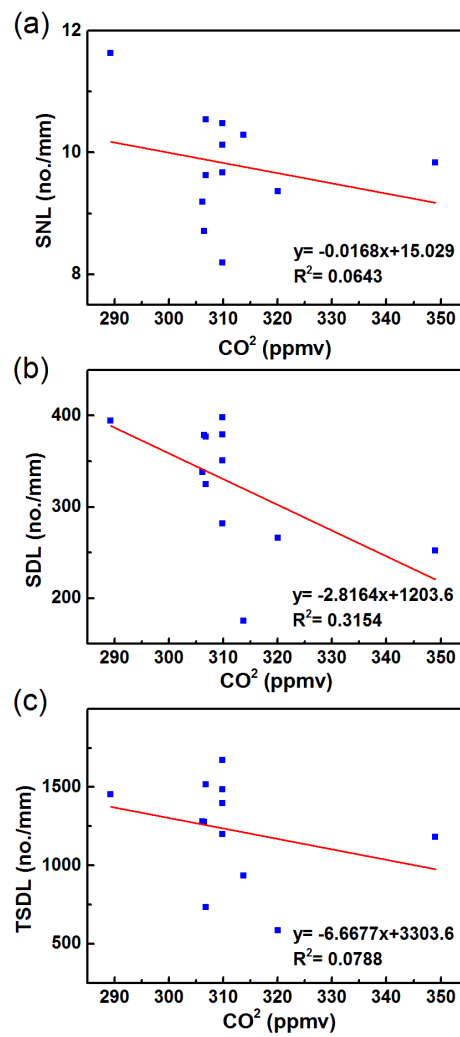


749 Figure 3. Correlation between SD and SI versus CO<sub>2</sub> concentration for modern *Nageia motleyi*. (a)  
 750 Trends of SD with CO<sub>2</sub> concentration for the adaxial surface. (b) Trends of SD with CO<sub>2</sub>  
 751 concentration for the abaxial surface. (c) Trends of SI with CO<sub>2</sub> concentration for the adaxial  
 752 surface. (d) Trends of SI with CO<sub>2</sub> concentration for the abaxial surface. (e) Trends of SD with  
 753 CO<sub>2</sub> concentration for the combined data of both leaf surfaces. (f) Trends of SI with CO<sub>2</sub>  
 754 concentration for the combined data of both leaf surfaces.



755  
 756

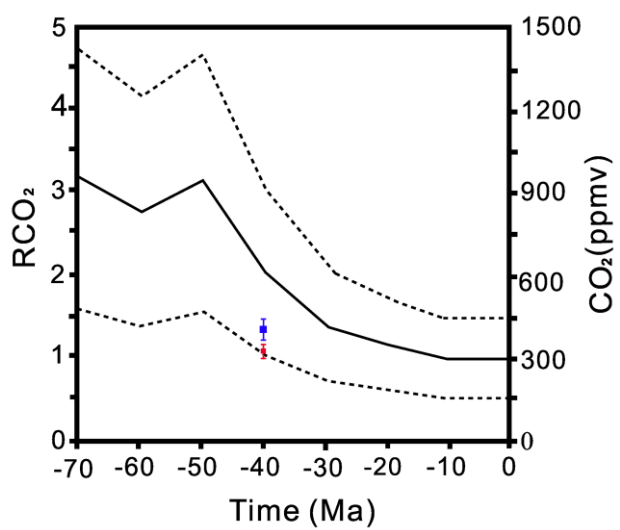
757 Figure 4. Correlation between SNL, SDL and TSDL versus CO<sub>2</sub> concentration for modern *Nageia*  
 758 *motleyi*. (a) Trends of SNL with CO<sub>2</sub> concentration for the adaxial surface. (b) Trends of SDL with  
 759 CO<sub>2</sub> concentration for the adaxial surface. (c) Trends of TSDL with CO<sub>2</sub> concentration for the  
 760 adaxial surface.



761

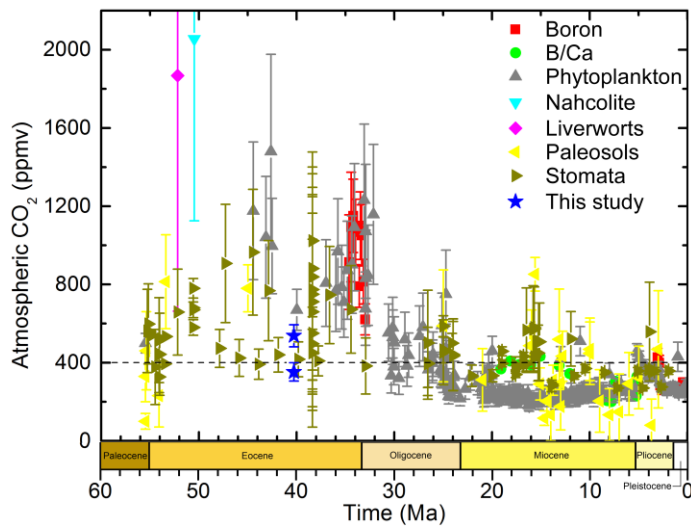
762

763 Figure 5. The pCO<sub>2</sub> reconstruction results and extant CO<sub>2</sub> concentrations are projected onto the  
764 long-term carbon cycle model (GEOCARB III; Berner and Kothaval á 2001). The pCO<sub>2</sub> results  
765 based on the regression approach and stomatal ratio method are represented by red and blue  
766 squares, respectively.



767  
768

769 Figure 6. Atmospheric CO<sub>2</sub> estimates from proxies over the past 60 million years. The horizontal  
770 dashed line indicates monthly atmospheric CO<sub>2</sub> concentration for March 2015 at Mauna Loa,  
771 Hawaii (401.5 ppmv) (Pieter and Keeling, 2015). The vertical lines show the error bars. The data  
772 are from the supporting data of Beerling and Royer (2011) and references in Table 9. The lower  
773 blue star shows the reconstructed result based on the regression approach. The higher one presents  
774 the result of stomatal ratio method.



776 Table 1. Modern *Nageia motleyi* (Parl.) De Laub samples and atmospheric CO<sub>2</sub> values of their collection dates from ice core data (Brown, 2010).  
777

Herbarium	Collection number	Collecting locality	Collectors	Number of leaf samples	Collection date	CO <sub>2</sub> (ppmv)
LE	No. 2649	Malaysia	Beccari, O.	1	1868	289.23
A/GH	No. bb. 17229	150 m, Riau on Ond. Karimon, Archipel. Ind.	Neth. Ind. For. Service	2	1932	306.19
A/GH	No. bb. 18328	5 m, Z. O. afd. v. Borneo Tidoengsche Landen, Archipel. Ind.	Neth. Ind. For. Service	2	1934	306.46
A/GH	No. bb. 21151	500 m, Z. O. afd. Borneo, Poeroek Tjahoe Tahoedjan, Archipel. Ind.	Neth. Ind. For. Service	2	1936	306.76
KEP	No. 30887	Kata Tinggi, Johor, Malaysia	Corner, E.J.H.	1	1936	306.76
KEP	No. 57329	Batang Padang, Perak, Malaysia	Unkonwn	2	1947	309.82
KEP	No. 57330	Batang Padang, Perak, Malaysia	Unkonwn	2	1947	309.82
KEP	No. 55897	Batang Padang, Perak, Malaysia	Unkonwn	2	1947	309.82
KEP	No. 61064	Batang Padang, Perak, Malaysia	Syed Woh	2	1947	309.82
E	No. bb. 40798	51 m, Kuala Trengganu-Besut Road, Bukit Bintang Block, Gunong Tebu Forest reserve, Malaysia	Sinclair, J. and Kiah bin, Salleh	2	1955	313.73
KEP	No. 80548	Gombak, Selangor, Malaysia	Rahim	1	1965	320.04
KEP	No. 33343	Jelebu, Negeri Sembilan, Malaysia	Yap, S.K.	2	1987	348.98

Note: A/GH—Harvard University Herbarium, Harvard University, 22 Divinity Avenue, Cambridge, Massachusetts 02138, USA ([www.huh.harvard.edu](http://www.huh.harvard.edu)).

E—The Herbarium of Royal Botanic Garden, Edinburgh EH3 5LR, Scotland, UK ([www.rbge.org.uk](http://www.rbge.org.uk)).

LE—The Herbarium of the V.L. Komarov Botanical Institute of the Russian Academy of Sciences, Prof. Popov Street 2, Saint Petersburg 197376, Russia ([www.binran.ru](http://www.binran.ru)).

KEP—Kepong Herbarium, Forest Research Institute Malaysia, 52109 Kepong, Selangor, Malaysia (<http://www.frim.gov.my/>).

778 Table 2. Summary of stomatal parameters of the adaxial surface from modern *Nageia motleyi* (Parl.) De Laub.

Collection number	Collection date	CO <sub>2</sub> (ppmv)	SD (mm <sup>-2</sup> )					SI (%)				
			$\bar{x}$	$\sigma$	s.e.	t*s.e.	n	$\bar{x}$	$\sigma$	s.e.	t*s.e.	n
No.2649	1868	289.23	78.60	15.44	1.41	2.76	120	3.44	0.66	0.06	0.12	120
No.bb.17229	1932	306.19	62.14	17.20	1.78	3.50	93	2.89	0.68	0.07	0.14	93
No.bb.18328	1934	306.46	64.57	15.05	1.58	3.11	90	3.39	1.01	0.11	0.21	90
No.bb.21151	1936	306.76	65.45	11.14	1.17	2.30	90	3.94	0.74	0.08	0.15	90
No.SFN30887	1936	306.76	66.90	16.10	1.27	2.49	161	3.61	0.92	0.07	0.14	161
No.61064	1947	309.82	56.71	16.81	1.95	3.83	74	3.27	1.26	0.15	0.29	74
No.57330	1947	309.82	67.37	15.97	2.04	4.01	61	3.70	0.82	0.10	0.20	61
No.57329	1947	309.82	67.85	15.61	1.70	3.34	84	3.50	0.90	0.10	0.20	84
No.55897	1947	309.82	66.74	14.10	1.78	3.48	63	3.18	0.66	0.08	0.16	63
No.40798	1955	313.73	45.89	13.81	1.12	2.20	151	3.03	0.87	0.07	0.14	151
No.KEP80548	1965	320.04	52.94	11.25	0.85	1.67	175	2.81	0.61	0.05	0.09	175
No.FRI33343	1987	348.98	52.25	12.05	0.77	1.51	242	2.87	0.69	0.04	0.09	242
Mean	—	—	62.28	14.54	1.45	2.85	117	3.30	0.52	0.08	0.16	117

*Note:*  $\bar{x}$ —mean;  $\sigma$ —standard deviation; s.e. —standard error of mean; n— numbers of photos counts (40×); t\*s.e.— 95% confidence interval.

779 Table 3. Summary of stomatal parameters of the abaxial surface from modern *Nageia motleyi* (Parl.) De Laub.

Collection number	Collection date	CO <sub>2</sub> (ppmv)	SD (mm <sup>-2</sup> )					SI (%)				
			<i>x</i>	$\sigma$	s.e.	t*s.e.	n	<i>x</i>	$\sigma$	s.e.	t*s.e.	n
No.2649	1868	289.23	82.71	12.23	1.02	2.00	144	3.89	0.58	0.05	0.09	144
No.bb.17229	1932	306.19	69.16	14.23	1.48	2.90	93	3.13	0.58	0.06	0.12	93
No.bb.18328	1934	306.46	69.92	14.38	1.52	2.97	90	3.99	1.08	0.11	0.22	90
No.bb.21151	1936	306.76	75.68	15.74	1.66	3.25	90	4.66	0.88	0.09	0.18	90
No.SFN30887	1936	306.76	76.18	12.51	0.99	1.93	161	4.42	0.89	0.07	0.14	161
No.61064	1947	309.82	60.93	11.02	1.39	2.72	63	3.05	0.62	0.08	0.15	63
No.57330	1947	309.82	75.82	14.14	1.82	3.58	60	4.38	0.84	0.11	0.21	60
No.57329	1947	309.82	71.74	16.84	1.75	3.42	93	3.72	0.62	0.06	0.13	93
No.55897	1947	309.82	78.63	13.41	1.75	3.42	59	4.41	1.00	0.13	0.26	59
No.40798	1955	313.73	53.22	13.88	1.12	2.19	155	3.71	0.93	0.07	0.15	155
No.KEP80548	1965	320.04	67.22	13.97	1.07	2.09	171	3.70	0.80	0.06	0.12	171
No.FRI33343	1987	348.98	59.09	12.10	0.79	1.55	233	3.69	0.86	0.06	0.11	233
Mean	—	—	70.03	13.70	1.36	2.67	118	3.90	0.81	0.08	0.16	118

*Note:* *x*—mean;  $\sigma$ —standard deviation; s.e. —standard error of mean; n— numbers of photos counts (40×); t\*s.e.— 95% confidence interval.

780

781 Table 4. Summary of stomatal parameters of the combined data of the adaxial and abaxial surfaces from modern *Nageia motleyi* (Parl.) De Laub.

Collection number	Collection date	CO <sub>2</sub> (ppmv)	SD (mm <sup>-2</sup> )					SI (%)				
			<i>x</i>	$\sigma$	s.e.	t*s.e.	n	<i>x</i>	$\sigma$	s.e.	t*s.e.	n
No.2649	1868	289.23	80.84	13.74	0.85	1.66	264	3.69	0.66	0.04	0.08	264
No.bb.17229	1932	306.19	65.65	16.13	1.18	2.32	186	3.01	0.64	0.05	0.09	186
No.bb.18328	1934	306.46	67.24	14.92	1.11	2.18	180	3.69	1.08	0.08	0.16	180
No.bb.21151	1936	306.76	70.57	14.53	1.08	2.12	180	4.30	0.89	0.07	0.13	180
No.SFN30887	1936	306.76	71.54	15.12	0.84	1.65	322	4.01	0.99	0.05	0.11	322
No.61064	1947	309.82	58.65	14.54	1.24	2.43	137	3.17	1.02	0.09	0.17	137
No.57330	1947	309.82	71.56	15.61	1.42	2.78	121	4.03	0.89	0.08	0.16	121
No.57329	1947	309.82	69.90	16.33	1.23	2.41	177	3.62	0.77	0.06	0.11	177
No.55897	1947	309.82	72.49	14.95	1.35	2.65	122	3.77	1.04	0.09	0.18	122
No.40798	1955	313.73	49.60	14.31	0.82	1.60	306	3.37	0.96	0.05	0.11	306
No.KEP80548	1965	320.04	60.00	14.53	0.78	1.53	346	3.25	0.84	0.05	0.09	346
No.FRI33343	1987	348.98	55.61	12.53	0.58	1.13	475	3.28	0.88	0.04	0.08	475
Mean	—	—	66.14	14.77	1.04	2.08	235	3.60	0.89	0.06	0.12	235

*Note:* *x*—mean;  $\sigma$ —standard deviation; s.e. —standard error of mean; n— numbers of photos counts (40 ×); t · s.e.— 95% confidence interval.

782



783 Table 5. Summary of stomatal parameters from modern *Nageia motleyi* (Parl.) De Laub (Kouwenberg et al., 2003).

Collection number	Collection date	CO <sub>2</sub> (ppmv)	SNL	SDL	TSDL	n
No.2649	1868	289.23	11.64	394.38	1455.10	264
No.bb.17229	1932	306.19	9.19	337.98	1280.12	186
No.bb.18328	1934	306.46	8.71	378.92	1277.63	180
No.bb.21151	1936	306.76	9.62	376.93	1517.21	180
No.SFN30887	1936	306.76	10.55	325.08	735.38	240
No.61064	1947	309.82	8.19	282.04	1200.66	133
No.57330	1947	309.82	9.67	397.83	1397.33	119
No.57329	1947	309.82	10.13	350.98	1672.50	176
No.55897	1947	309.82	10.48	379.06	1486.13	122
No.40798	1955	313.73	10.29	175.14	933.85	305
No.KEP80548	1965	320.04	9.36	266.16	585.72	263
No.FRI33343	1987	348.98	9.84	252.20	1181.51	125
Mean	–	–	9.81	326.39	1226.93	191

784

785

786

787 Table 6. Summary of stomatal parameters of the adaxial surface of fossil *Nageia* and pCO<sub>2</sub> [*C<sub>f</sub>*] estimates results.

Species	Age	SD (mm <sup>-2</sup> )				SI (%)				SR		pCO <sub>2</sub> (ppmv)		<i>C<sub>f</sub></i> (ppmv)	
		<i>x</i>	$\sigma$	s.e.	n	<i>x</i>	$\sigma$	s.e.	n	<i>x</i>	t*s.e	<i>x</i>	t*s.e	<i>x</i>	t*s.e
MMJ1-001	Late Eocene	52.5	17.1	3.1	30	2.08	0.7	0.1	30	1.35	0.19	333.6	13.9	412.1	62.0
MMJ2-003	Late Eocene	42.3	12.9	2.4	30	1.80	0.6	0.1	30	1.75	0.39	356.8	10.5	536.1	126.2
MMJ2-004	Late Eocene	39.9	13.6	2.5	30	1.66	0.6	0.1	30	1.81	0.32	362.4	11.0	554.3	101.9
MMJ3-003a	Late Eocene	43.2	17.7	3.2	30	1.67	0.7	0.1	30	1.84	0.43	354.8	14.4	564.6	135.7
Mean	Late Eocene	44.5	16.3	1.5	120	1.80	0.7	0.1	120	1.69	0.18	351.9	6.6	516.8	56.5

Note: *x*—mean;  $\sigma$ —standard deviation; s.e. —standard error of mean; n— numbers of photos counts (400×); t\*s.e.— 95% confidence interval. pCO<sub>2</sub>— the result based the regression approach; *C<sub>f</sub>*— the result based on the stomatal method.

788

789

790 Table 7. Summary of stomatal parameters of the abaxial surface of fossil *Nageia* and pCO<sub>2</sub> [*C<sub>f</sub>*] estimates results.

Species	Age	SD (mm <sup>2</sup> )				SI (%)				SR		pCO <sub>2</sub> (ppmv)		<i>C<sub>f</sub></i> (ppmv)	
		<i>x</i>	$\sigma$	s.e.	n	<i>x</i>	$\sigma$	s.e.	n	<i>x</i>	t*s.e	<i>x</i>	t*s.e	<i>x</i>	t*s.e
MMJ1-001	Late Eocene	47.7	17.7	3.2	30	2.11	0.8	0.2	30	1.66	0.23	368.6	16.2	515.6	72.3
MMJ2-003	Late Eocene	50.9	18.3	3.3	30	2.12	0.8	0.1	30	1.57	0.23	360.9	16.6	486.0	70.7
MMJ2-004	Late Eocene	48.2	15.8	2.9	30	2.14	0.7	0.1	30	1.63	0.25	367.4	14.5	504.6	77.3
MMJ3-003a	Late Eocene	48.9	12.6	2.7	22	1.85	0.5	0.1	22	1.52	0.19	365.4	13.5	472.3	59.0
Mean	Late Eocene	48.9	16.2	1.5	112	2.07	0.7	0.1	112	1.60	0.11	365.6	7.6	496.1	35.7

*Note:* *x*—mean;  $\sigma$ —standard deviation; s.e. —standard error of mean; n— numbers of photos counts (400 $\times$ ); t\*s.e.— 95% confidence interval. pCO<sub>2</sub>— the result based the regression approach; *C<sub>f</sub>*— the result based on the stomatal method.

791

792 Table 8. Summary of stomatal parameters of the combined data of the adaxial and abaxial surfaces of fossil *Nageia* and pCO<sub>2</sub> [*C*<sub>(f)</sub>] estimates  
 793 results.

Species	Age	SD (mm <sup>-2</sup> )				SI (%)				SR		pCO <sub>2</sub> (ppmv)		<i>C</i> <sub>(f)</sub> (ppmv)	
		<i>x</i>	$\sigma$	s.e.	n	<i>x</i>	$\sigma$	s.e.	n	<i>x</i>	t*s.e	<i>x</i>	t*s.e	<i>x</i>	t*s.e
MMJ1-001	Late Eocene	50.1	17.5	2.3	60	2.09	0.8	0.1	60	1.50	0.15	349.7	10.6	471.2	47.8
MMJ2-003	Late Eocene	46.5	16.3	2.1	60	1.96	0.7	0.1	60	1.67	0.24	358.3	9.8	524.1	75.7
MMJ2-004	Late Eocene	44.0	15.8	2.0	60	1.90	0.7	0.1	60	1.73	0.17	364.3	9.5	542.9	52.6
MMJ3-003a	Late Eocene	45.6	16.1	2.2	52	1.75	0.6	0.1	52	1.73	0.28	360.5	10.4	544.6	88.3
Mean	Late Eocene	46.6	16.4	1.1	232	1.93	0.7	0.1	232	1.66	0.11	358.1	5.0	519.9	35.0

*Note:* *x*—mean;  $\sigma$ —standard deviation; s.e. —standard error of mean; n— numbers of photos counts (400×); t\*s.e.— 95% confidence interval. pCO<sub>2</sub>— the result based the regression approach; *C*<sub>(f)</sub>— the result based on the stomatal method.

794

795 Table 9. pCO<sub>2</sub> estimates proxies and corresponding references.

Proxies	References
Boron	Pearson et al., 2009; Seki et al., 2010
B/Ca	Tripathi et al., 2009
Phytoplankton	Freeman and Hayes, 1992; Stott, 1992; Pagani et al., 1999, 2005; Henderiks and Pagani, 2008; Seki et al., 2010
Nahcolite	Lowenstein and Demicco, 2006
Liverworts	Fletcher et al., 2008
Paleosols	Cerling, 1992; Koch et al., 1992; Ekart et al., 1999; Royer et al., 2001; Nordt et al., 2002; Retallack, 2009b; Huang et al. 2013
Stomata	Van der Burgh et al., 1993; Kürschner et al., 1996, 2001, 2008; McElwain, 1998; Royer et al., 2001, 2003; Greenwood et al., 2003; Beerling et al., 2009; Retallack, 2009a; Smith et al., 2010; Doria et al., 2011; Roth-Nebelsick et al., 2012; 2014; Grein et al., 2013; Maxbauer et al., 2014

796